Plasminogen activator inhibitor-1 polymers, induced by inactivating amphipathic organochemical ligands

Katrine E. PEDERSEN*[1], Anja P. EINHOLM*, Anni CHRISTENSEN*, Lotte SCHACK*, Troels WIND*, John M. KENNEY† and Peter A. ANDREASEN*

*Department of Molecular Biology, University of Aarhus, Gustav Wieds Vej 10, DK-8000 Aarhus C, Denmark, and †Institute for Storage Ring Facilities, University of Aarhus, Ny Munkegade 525, DK-8000 Aarhus C, Denmark

Negatively charged organochemical inactivators of the anti-proteolytic activity of plasminogen activator inhibitor-1 (PAI-1) convert it to inactive polymers. As investigated by native gel electrophoresis, the size of the PAI-1 polymers ranged from dimers to multimers of more than 20 units. As compared with native PAI-1, the polymers exhibited an increased resistance to temperature-induced unfolding. Polymerization was associated with specific changes in patterns of digestion with non-target proteases. During incubation with urokinase-type plasminogen activator, the polymers were slowly converted to reactive centre-cleaved monomers, indicating substrate behaviour of the terminal PAI-1 molecules in the polymers. A quadruple mutant of PAI-1 with a retarded rate of latency transition also had a retarded rate of polymerization. Studying a number of serpins by native gel electrophoresis, ligand-induced polymerization was observed only with PAI-1 and heparin cofactor II, which were also able to copolymerize. On the basis of these results, we suggest that the binding of ligands in a specific region of PAI-1 leads to so-called loop–sheet polymerization, in which the reactive centre loop of one molecule binds to β-sheet A in another molecule. Induction of serpin polymerization by small organochemical ligands is a novel finding and is of protein chemical interest in relation to pathological protein polymerization in general.

Key words: cancer, polymerization, serpin, thrombosis, urokinase.

INTRODUCTION

The serpins constitute a family of globular proteins with a unique conformational flexibility, having as a common theme the insertion of the surface-exposed reactive centre loop (RCL) as strand 4 of the large central β-sheet A (see Figure 1A). The insertion results in a considerable thermodynamic stabilization of the molecule. Hence, forms with an inserted RCL are referred to as 'relaxed' (R), and those with an exposed RCL as 'stressed' (S) [1]. The best known members of the serpin family are inhibitors of mammalian serine proteases (hence the name; reviewed in [2–6]). The stabilization associated with RCL insertion is the basis for the serpin inhibitory mechanism. Serpins inhibit their target proteases by presenting the P_1-P'_1 bond in the RCL to the protease active site [7]. Following formation of the acyl enzyme intermediate, however, the release of P_1 from P'_1 allows the serpin to become stabilized by insertion of the N-terminal part of the RCL as β-strand 4A (s4A). The active-site Ser of the protease now being covalently bound to the carboxy group of the P_1 residue of the serpin by an ester bond, the insertion implies a translocation of the protease to the pole of the serpin molecule opposite to that of its initial encounter with the protease. Concomitantly, the active site of the protease is distorted and the catalytic machinery inactivated, halting hydrolysis of the ester bond and resulting in formation of a stable complex [8–13]. In some cases, when RCL insertion is delayed, protease distortion becomes too slow to prevent ester bond hydrolysis, resulting in release of an active protease and a P_1-P'_1-bond-cleaved serpin with a fully inserted N-terminal part of the RCL. In these cases, the serpin is said to exhibit substrate behaviour [14]. RCL insertion implies a re-arrangement of a buried hydrogen-bonding network in the so-called shutter region, involving residues 53 and 56 in α-helix B (hB) and residue 334 in s5A {the numbering of plasminogen activator inhibitor-1 (PAI-1) used in this report corresponds to the α_1-proteinase inhibitor template numbering according to [2]}. In addition, the expansion of β-sheet A results in a narrowing of the space between s2A and helices D and E (hD and hE) in the so-called flexible joint region (see Figure 1A; reviewed in [6]).

The tendency of the RCL of serpins to become an additional strand in a pre-existing β-sheet also makes them prone to other types of loop-sheet interactions. A type of RCL insertion first discovered with the serpin PAI-1 is conversion to the inactive, so-called latent form, in which the RCL's N-terminal part is inserted as s4A and its C-terminal part is stretched out along the surface of the molecule [15]. Premature β-sheet expansion in serpins can also result in polymerization. There is evidence for three different modes of loop–sheet polymerization (Figure 1B). First, based on observation of dimers in crystals of antithrombin III, the RCL of one molecule can insert as s1C in another molecule, in which the intrinsic s1C has been extracted [16–18]. Second, based on observation of dimers in crystals of PAI-1, the RCL of one molecule can hydrogen bond to s6A of another molecule and thus form a s7A [19–21]. Thirdly, heating or mutations in the shutter region can lead to polymerization believed to involve insertion of the RCL of one molecule as s4A of another molecule (reviewed in [22]). This kind of polymer was

Abbreviations used: 1-DS, 1-dodecyl sulphuric acid; α_1-ACT, α_1-antichymotrypsin; α_1-PI, α_1-proteinase inhibitor; ANS, 8-anilinonaphthalene-1-sulphonic acid; bis-ANS, 4,4′-dianilino-1,1′-bisnaphthyl-5,5′-disulphonic acid; HBS, Hepes-buffered saline; HCII, heparin cofactor II; HEK293, human embryonic kidney 293T cell line; hB, α-helix B (etc.); HMK, heart muscle kinase; PAI-1, plasminogen activator inhibitor-1; R, relaxed form; RCL, reactive-centre loop; s, β-strand; S, stressed form; S-2444, L-5-pyroglutamyl-glycyl-L-arginine-*p*-nitroaniline; TCA, trichloroacetic acid; TVASS, acetyl-Thr-Val-Ala-Ser-Ser-NH_2 peptide; uPA, urokinase-type plasminogen activator; wt, wild type.

[1] To whom correspondence should be addressed (e-mail kep@mb.au.dk).

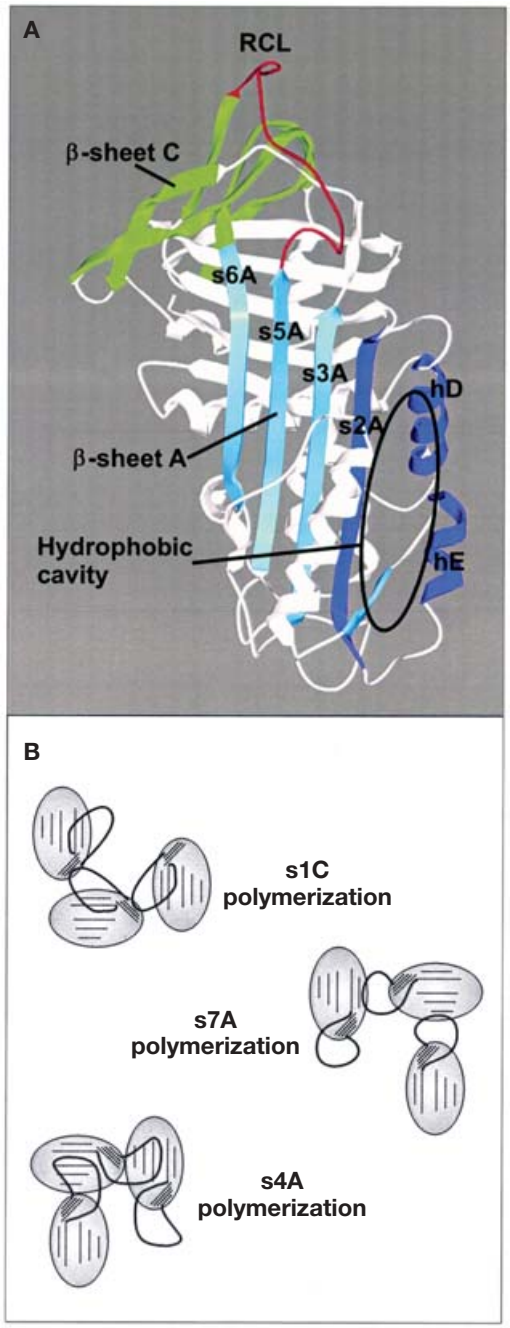

Figure 1 Three-dimensional structure of PAI-1 in the active conformation

(**A**) The molecule is a representation of co-ordinates given in the Protein Data Bank (accession no. 1DB2). The RCL is shown in red, the central β-sheet A in light blue, and β-sheet C in green. The secondary structural elements surrounding the hydrophobic, ligand-binding cavity are shown in dark blue. (**B**) Schematic of three different mechanisms of serpin polymerization.

observed in crystals of cleaved α_1-proteinase inhibitor (α_1-PI) [23,24].

Recently, we described a novel way of inducing polymerization in serpins. The flexible joint region of PAI-1 and a few other serpins contains a hydrophobic cavity between s2A and hD and hE (Figure 1A). The cavity is considerably larger in active PAI-1 than in the forms with an inserted RCL [19–21,25]. Accordingly, surface plasmon resonance [26] and fluorimetric binding [27] assays indicated that the binding of inactivating amphipathic compounds was much stronger to active PAI-1 than to the RCL-inserted forms. The cavity binds a variety of structurally diverse compounds, including ANS (8-anilinonaphthalene-1-sulphonic acid), AR-H029953XX {*N*-[*N*-(3,4-dichlorophenyl)benzamide] anthranilic acid}, bis-ANS (4,4′-dianilino-1,1′-bisnaphthyl-5,5′-disulphonic acid), and 1-dodecyl sulphuric acid (1-DS), with K_d values between 0.5 and several hundred micromolar [27]. We discovered that the negatively charged organochemical compounds induce substrate behaviour, followed by conversion of PAI-1 to inactive, polymeric forms [27]. We have now undertaken a biochemical characterization of the inactivator-induced PAI-1 polymers.

EXPERIMENTAL

PAI-1

Natural human PAI-1 was purified from conditioned medium of dexamethasone-treated HT-1080 cells [28]. Recombinant glycosylated human PAI-1, either unmodified wild type (wt), the quadruple variant N171H-K175T-Q331L-M366I [29] (referred to as 'stable PAI-1'), or PAI-1 N-terminally extended with the target sequence Arg-Arg-Ala-Ser-Val for heart muscle kinase (HMK; referred to as HMK-PAI-1), was expressed using the pcDNA3.1(–) PAI-1 vector [30]. HMK-PAI-1 cDNA was constructed from the pcDNA3.1(–)PAI-1 vector by insertion of the Arg-Arg-Ala-Ser-Val sequence between the signal sequence and the mature protein sequence. Additionally, the signal peptide cleavage site was optimized in positions –1 and –3 [31], by changing the two glycine residues in these positions to alanine residues, to prevent cleavage in the Arg-Arg-Ala-Ser-Val sequence in the position used in natural PAI-1. The cDNA constructs were transiently transfected into human embryonic kidney 293T (HEK293) cells by the calcium phosphate precipitation method [30] and purified in the latent form from the serum-free medium [28]. N-terminal sequencing confirmed that the purified HMK-PAI-1 had the expected N-terminal sequence Arg-Arg-Ala-Ser-Val-His-His-Pro-Pro-Ser. All purified latent PAI-1 variants were activated by denaturation with 4 M guanidinium chloride, followed by refolding by dialysis against Hepes-buffered saline (HBS; 10 mM Hepes, pH 7.4, 140 mM NaCl).

Recombinant non-glycosylated PAI-1 from *Escherichia coli* with a hexa-His tag and HMK sequence was expressed and purified in the active form [32].

HMK-catalysed ^{32}P-labelling of HMK-PAI-1 at the serine residue in the recognition sequence Arg-Arg-Ala-Ser-Val was performed as described previously [33]. The ^{32}P-labelled PAI-1 had a specific radioactivity of approx. 2000 Ci/mmol.

Miscellaneous materials

Urokinase-type plasminogen activator (uPA) was purchased from Wakamoto (Tokyo, Japan). Elastase, endoproteinase Asp-N, endoproteinase Glu-C, endoproteinase Lys-C, and papain were purchased from Roche Diagnostics (Mannheim, Germany). Subtilisin Carlsberg was purchased from Sigma–Aldrich (St. Louis, MO, U.S.A.). Antithrombin III and C1-inhibitor were gifts from the late Professor S. Magnusson (Department of Molecular Biology, University of Aarhus, Denmark). Recombinant human Pittsburgh variant of α_1-PI was a gift from Dr A. Zhou (Department of Haematology, University of Cambridge, U.K.). PAI-2 was a gift from Professor P. H. Jensen (Department of Medical Biochemistry, Aarhus University, Denmark). Chicken ovalbumin was from Sigma–Aldrich. Heparin cofactor II (HCII)

was a gift from Professor P. Sié (Laboratoire d'Hemostase, Centre de Transfusion Sanguine CHU Purpan, Toulouse, France). α_1-Antichymotrypsin (α_1-ACT) and α_2-antiplasmin were gifts from Professor J. Enghild (Department of Molecular Biology, University of Aarhus, Denmark). Acetyl-Thr-Val-Ala-Ser-Ser-NH_2 (TVASS) was purchased from Medprobe (Oslo, Norway). The following chemicals were purchased from the indicated sources: ANS (Sigma–Aldrich); bis-ANS (Molecular Probes, Eugene, OR, U.S.A.); porcine gelatine (Sigma–Aldrich); sodium salt of 1-DS (Merck); L-5-pyroglutamyl-glycyl-L-arginine-*p*-nitroaniline (S-2444) (Chromogenix, Mölndal, Sweden). All other materials were of the best grade available.

Native PAGE

The electrophoresis was performed in 5–15 % (w/v) polyacrylamide gels, with 0.02 % (w/v) Coomassie Blue in the cathode buffer [27,34]. Upon lengthy electrophoresis, the PAI-1 monomer band partly separated into active and latent species.

Measurement of PAI-1 solubility in the absence or presence of inactivator

For determination of solubility of PAI-1 at different PAI-1 concentrations, 100 pM ^{32}P-labelled HEK293 PAI-1 or ^{32}P-labelled *E. coli* PAI-1 was supplemented with non-radioactive PAI-1 from the same expression system at different concentrations. For determination of solubility at different NaCl concentrations, 100 pM ^{32}P-labelled HEK293 PAI-1 or *E. coli* PAI-1 was supplemented with unlabelled PAI-1 from the same expression system to a concentration of 0.4 μM in 10 mM Hepes, pH 7.4, with different concentrations of NaCl. For both assays, the samples were incubated for 60 min at 37 °C in the absence or presence of 100 μM 1-DS. The samples were then centrifuged at 10000 ***g*** for 10 min at 4 °C and the radioactivity left in solution was determined by scintillation counting of aliquots from the supernatants.

Analysis of functional behaviour of PAI-1 by reaction with uPA and SDS/PAGE

After various incubations in HBS, unlabelled and ^{32}P-labelled HEK293 PAI-1 at a final total concentration of 2 μM was mixed with 2 μM uPA. For 1440 min incubations with uPA, the samples were supplemented with 3 μg/ml trasylol. After a reaction period as indicated for each experiment, the samples were made 2 % (w/v) with respect to SDS and subjected to SDS/PAGE in 11 % polyacrylamide gels. [^{32}P]PAI-1 was visualized by autoradiography. This analysis separates PAI-1 as inhibitory active, i.e. as a complex with uPA; as exhibiting substrate behaviour, i.e. as the reactive-centre-cleaved form, where only the large N-terminal fragment will be recovered by the conditions used; and as inert PAI-1, such as the latent form, i.e. co-migrating with native PAI-1.

Measurement of thermal stability of PAI-1 and α_1-PI

Samples of PAI-1 (4 μM) in HBS were incubated for 60 min at 37 °C with 100 μM 1-DS or at 0 °C without additions. The different PAI-1 samples were then incubated at different temperatures for 2 h at the same concentration. After incubation, the samples were cooled on ice and centrifuged at 10000 ***g*** for 10 min. Aliquots from the supernatants were subjected to SDS/PAGE in 6–16 % polyacrylamide gels and stained with Coomassie Blue. The intensities of the bands were quantified using ImageQuant software version 3.3 (Molecular Dynamics, Sunnyvale, CA, U.S.A.) and expressed relative to the intensity of the band corresponding to PAI-1 incubated at 0 °C. α_1-PI polymers were induced by incubating 5 μM α_1-PI for 180 min at 62 °C. The thermal stability of these polymers was determined as for PAI-1, in parallel with α_1-PI preincubated at 0 °C for 180 min.

Analysis of PAI-1 polymers by limited proteolysis

PAI-1 (6 μM) in HBS was incubated for 60 min at 37 °C with 100 μM 1-DS or at 0 °C without additions. The samples were then diluted with HBS to a PAI-1 concentration of 0.4 μM. Proteases were added in concentrations between 0.1 and 1 μg/ml. For digestions with papain, the buffer was supplemented with 0.5 mM cysteine and 0.1 mM EDTA. Digestions were stopped by addition of trichloroacetic acid (TCA) to 7 % (w/v). Cleavage sites were determined by N-terminal sequencing of the TCA-precipitates on an Applied Biosystems 477A Sequencer. New sequences caused by proteolytic cleavages appeared at a yield of 50–100 % as compared with the original N-terminus, except for papain and subtilisin, in which cases the sequences of the cleavage products appeared at a yield of only approx. 25 %.

Fluorimetric binding assays

Fluorescence emission spectra of bis-ANS were recorded with an SFM 25 spectrofluorimeter (Kontron Instruments, Watford, Herts., U.K.) with excitation wavelength 395 nm. The emission was recorded over the range 400–600 nm. In standard measurements, 1 μM PAI-1 and 4 μM bis-ANS in HBS were used. The operating temperature was 37 °C.

Measurement of the incorporation rate of TVASS in PAI-1

The specific inhibitory activity of PAI-1 after incubation with TVASS for different time periods was measured by titration against uPA in a peptidyl anilide assay. Briefly, 1 μM PAI-1 was pre-incubated with 250 μM TVASS. At regular time intervals, samples were withdrawn and serially diluted in HBS with 0.25 % (w/v) gelatine at 37 °C to final concentrations between 0.2–200 nM. uPA was then added to a final concentration of 5 nM. The final volume was 200 μl. The incubation was continued for 5 min. Residual uPA activity was determined by addition of the peptidyl anilide substrate S-2444 and measurement of the increase in absorbance at 405 nm. The activity of PAI-1 was calculated from the amount of PAI-1 that inhibited 50 % of the added uPA. The half-life of the functional activity was calculated from a semi-logarithmic plot of specific inhibitory activity versus time.

Molecular graphics

A SwissPDB viewer [35] was used to display the three-dimensional structure of active PAI-1 [20].

RESULTS

We previously demonstrated that inactivation of PAI-1 in micromolar concentrations by negatively charged organochemicals proceeds in two consecutive steps. First, within seconds, active PAI-1 is converted to a form exhibiting substrate behaviour,

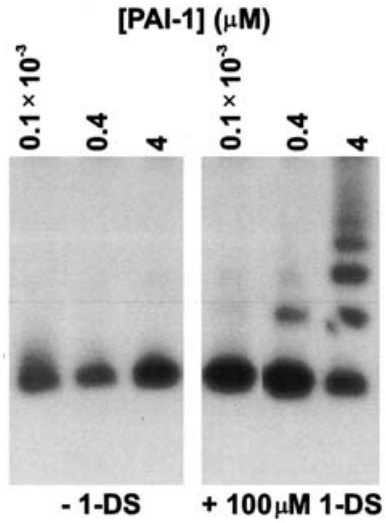

Figure 2 Effect of the PAI-1 concentration on the rate of polymerization

^{32}P-labelled HEK293 PAI-1 (100 pM) and various concentrations of unlabelled HEK293 PAI-1, with the indicated total concentrations, were incubated for 30 min in the absence or presence of 100 μM 1-DS at 37 °C. The samples were then subjected to native PAGE. The [^{32}P]PAI-1 was visualized by autoradiography.

i.e. it is cleaved by uPA in less than 2 min. Secondly, within 10 min, PAI-1 is converted into inert polymers [27]. We have now analysed the polymerization reaction by native PAGE, using [^{32}P]PAI-1 in order to analyse polymerization at low PAI-1 concentrations. Without exposure to inactivators, PAI-1 migrated mainly as a monomer in the position expected relative to the molecular mass markers (Figure 2). Exposing 100 pM [^{32}P]PAI-1 to 1-DS did not lead to polymerization, but the polymerization rate clearly increased on adding non-radioactive PAI-1 to increase the total PAI-1 concentration. With an incubation time of 30 min, there was no detectable polymerization at PAI-1 concentrations below 0.4 μM, and the degree of polymerization was increased markedly by increasing the PAI-1 concentration from 0.4 to 4 μM (Figure 2). The polymers consisted of distinct bands, which by comparison with the markers, seemed to represent dimers, trimers, tetramers, etc. The gel system did not allow resolution of polymer species with a molecular mass above approx. 250 000 Da. Similar findings were obtained with ANS- and bis-ANS-induced inactivation (results not shown). The inactivators did not induce polymerization of latent and reactive centre-cleaved PAI-1 (results not shown).

If not indicated otherwise, our experiments were all performed with glycosylated PAI-1 from HEK293T cells or HT-1080 cells. PAI-1 expressed in *E. coli*, i.e. non-glycosylated, also polymerizes when exposed to the negatively charged inactivators [27]. However, non-glycosylated PAI-1 in concentrations above approx. 1 μM precipitated when exposed to polymerization-inducing inactivators. Also, polymerization-inducing ligands caused precipitation of even lower concentrations of non-glycosylated PAI-1 when the salt concentration was increased above physiological levels, whereas polymerization and solubility of glycosylated PAI-1 was not affected by salt concentrations of up to 1 M (results not shown).

We characterized the reaction of the 1-DS-induced inhibitory inactive polymeric PAI-1 with uPA by native PAGE and SDS/PAGE (Figure 3). Without incubation with inactivator, more than 50 % of denatured and refolded PAI-1 was in the active conformation, whereas the rest was either recovered as inert, probably latent PAI-1, or exhibited substrate behaviour. After

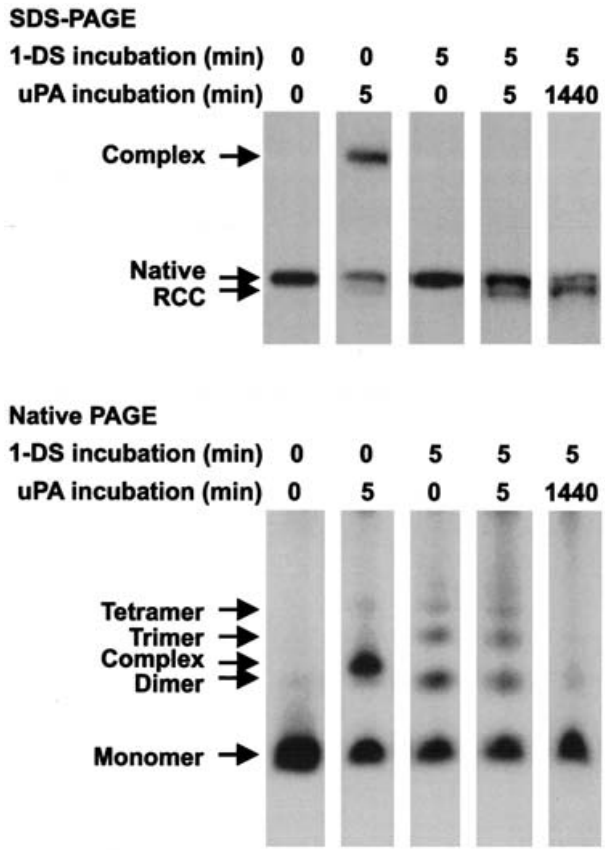

Figure 3 Depolymerization of PAI-1 during prolonged incubation with uPA

HEK293 PAI-1 (2 μM), including 100 pM ^{32}P-labelled HEK293 PAI-1, was incubated for different time periods at 37 °C with 50 μM 1-DS before addition of 2 μM uPA or buffer, as indicated. The incubation was then continued at 37 °C for the indicated time periods. Samples were subjected to SDS/PAGE or native PAGE, as indicated. [^{32}P]PAI-1 was visualized by autoradiography. RCC, reactive centre-cleaved.

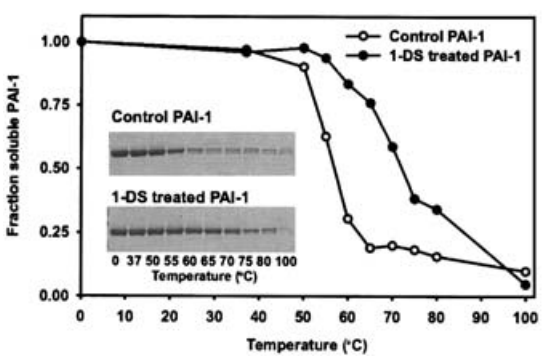

Figure 4 Thermal stability of PAI-1 polymers

Samples of HT-1080 PAI-1 (6 μM) were or were not incubated with 100 μM 1-DS for 60 min at 37 °C. The samples were then incubated at different temperatures for a further 2 h, followed by centrifugation. The supernatants were subjected to SDS/PAGE. The gels were stained with Coomassie Blue. The intensities of the PAI-1 bands were expressed relative to that representing PAI-1 incubated at 0 °C. The temperatures leading to precipitation of half of the active monomeric PAI-1 and polymerized PAI-1 were determined from the curve as 57 and 72 °C respectively.

5 min incubation with 1-DS, most PAI-1 was converted to inactive polymers, which showed little or no substrate behaviour but were largely inert to a 5 min incubation with uPA. However, extended incubation of polymeric PAI-1 with uPA resulted in most PAI-1

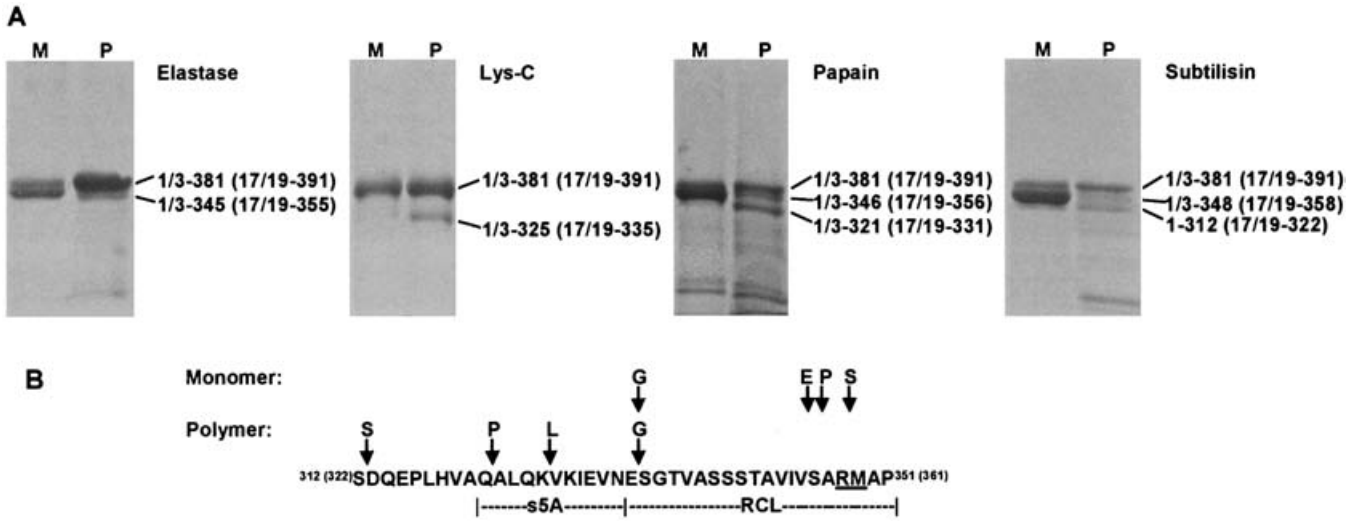

Figure 5 Proteolytic susceptibility of monomeric and polymeric PAI-1

(**A**) Monomeric active (M) or polymeric inactive (P) HT-1080 PAI-1 was subjected to limited proteolysis at 37 °C with 1 μg/ml elastase for 30 min, 1 μg/ml endoproteinase Lys-C for 10 min, 1 μg/ml papain for 30 min, or 0.2 μg/ml subtilisin for 5 min. Samples were then TCA-precipitated and subjected to SDS/PAGE. The gels were stained with Coomassie Blue. Identified fragments are indicated next to the gel, with PAI-1 numbering according to [51]. Numbers in parentheses are according to the α_1-PI template numbering [1]. It should be noted that cleavage products below 15 kDa will not be recovered by the gel system in use, but are present in the TCA-precipitates and can thus be identified by N-terminal sequencing. (**B**) Primary sequence of the s5A–RCL (residues 322–361) stretch in PAI-1. Corresponding secondary structural elements [3] are indicated below the sequence. The reactive centre is underlined. Utilized cleavage sites in monomers and polymers are shown with arrows above the sequence: P, papain; E, elastase; S, subtilisin; G, endoproteinase Glu-C; L, endoproteinase Lys-C.

being cleaved in the reactive centre, complete cleavage requiring more than 1440 min. During the prolonged incubation with uPA, the polymers slowly depolymerized. Polymers incubated without uPA did not become cleaved in the reactive centre and did not depolymerize (results not shown). Thus prolonged exposure of the polymers to uPA causes depolymerization concomitantly with reactive centre cleavage.

Polymerized PAI-1 showed a 15 °C increased resistance to temperature-induced precipitation as compared with monomeric, active PAI-1 (Figure 4). The polymers were, however, not as stable as reactive-centre-cleaved PAI-1, which remains in solution at temperatures of up to 100 °C [36]. In comparison, polymers of α_1-PI were, in agreement with previous work [37], found to remain in solution at temperatures above 90 °C (results not shown).

We used the strategy of measuring proteolytic susceptibility of specific peptide bonds to map conformational changes of PAI-1 in association with conversion to polymers. Active monomeric and inactive polymeric PAI-1 were incubated with proteases for various time periods. The digestions were stopped by TCA precipitation. The digestion patterns were analysed by SDS/PAGE and N-terminal sequence analysis of the TCA precipitates (Figure 5). We observed changes in the susceptibility of specific peptide bonds to elastase, endoproteinase Lys-C, papain, and subtilisin.

Elastase cleaved the P_4–P_3 bond of the RCL of active, monomeric PAI-1. After polymerization, the yield of the fragment corresponding to this cleavage site was strongly reduced and no other major cleavages occurred.

Endoproteinase Lys-C has no potential cleavage sites in the RCL. Active, monomeric PAI-1 was virtually resistant to endoproteinase Lys-C, but polymerization induced a new cleavage site, which was localized to the Lys^{335}-Val^{336} bond in s5A using N-terminal sequencing.

Papain cleaved the P_3-P_2 bond of the RCL of active, monomeric PAI-1. After polymerization, the fragment corresponding to this cleavage site was almost undetectable, and polymerized PAI-1 displayed a generally increased susceptibility to papain. A fragment corresponding to cleavage of the Gln^{331}–Ala^{332} bond in s5A became a predominant cleavage product. Other fragments appeared in lower yield, and we did not attempt to identify them.

Subtilisin cleaved the P_1–P_1' bond of the RCL of active, monomeric PAI-1. After polymerization, the fragment corresponding to this cleavage site could not be distinguished, and

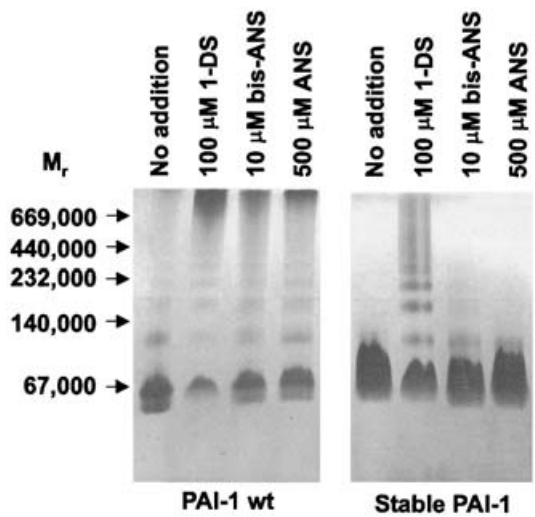

Figure 6 Polymerization of stable PAI-1

HEK293 PAI-1 wt or stable variant (6 μM) was incubated for 30 min at 37 °C with or without 100 μM 1-DS, 500 μM ANS or 10 μM bis-ANS, as indicated. Samples (10 μg) were then subjected to native PAGE and visualized with Coomassie Blue. The 1-DS-induced wt-polymers migrated at the top of the gel, corresponding to a molecular mass of $>$ 669 000 DA.

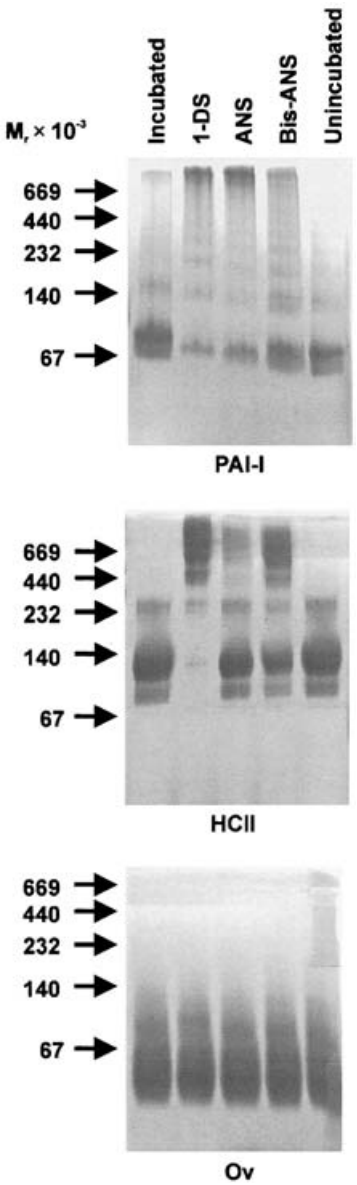

Figure 7 Effects of ANS, bis-ANS and 1-DS on PAI-1, HCII and ovalbumin, as investigated by native PAGE

HT-1080 PAI-1, HCII or ovalbumin (Ov) (each at a concentration of 6 μM) was incubated for 30 min at 37 °C with 100 μM 1-DS, 500 μM ANS, 10 μM bis-ANS or without additions. An unincubated sample was also included. Samples (10 μg) were then subjected to native PAGE.

polymerized PAI-1 had a generally increased susceptibility to subtilisin. A fragment corresponding to cleavage of the Ser^{322}–Asp^{323} bond in the loop connecting hI and s5A became a new cleavage product in polymerized PAI-1 samples. Identification of the other minor cleavage products was not attempted.

Endoproteinase Asp-N cleaved active, monomeric PAI-1 at a few specific bonds, which we previously localized to the flexible joint region [38]. There were no clear changes in the cleavage patterns following polymerization (results not shown). It should be noted that there are no potential cleavage sites for endoproteinase Asp-N in the RCL or s5A of PAI-1. Endoproteinase Glu-C was previously reported to cleave the Glu^{342}–Ser^{343} (P_{17}–P_{16}) bond of active, but not latent, PAI-1 [39].

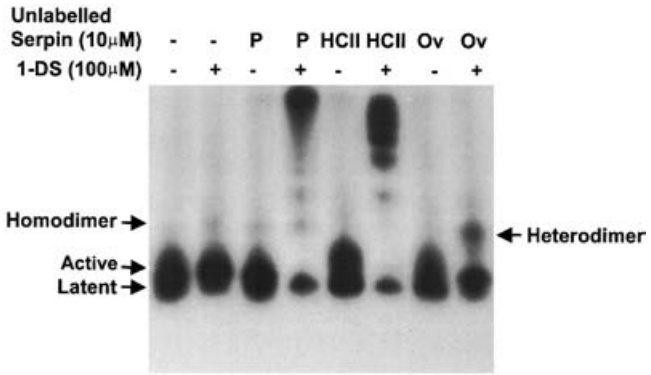

Figure 8 Co-polymerization of PAI-1 with other serpins

^{32}P-labelled HEK293 PAI-1 (100 pM) was mixed with either 0 or 100 μM 1-DS in the absence or presence of 10 μM unlabelled HEK293 PAI-1 (P), HCII, or ovalbumin (Ov), as indicated, and incubated for 30 min at 37 °C. The samples were then subjected to native PAGE. The [^{32}P]PAI-1 was visualized by autoradiography.

Polymerization of PAI-1 did not lead to changes in this cleavage. No further major cleavages were observed (results not shown).

Thus the investigations gave a consistent picture of cleavages in the RCL being inhibited and replaced by cleavage sites in the sequence 322–335.

Stable PAI-1, i.e. PAI-1 with the quadruple substitution N171H-K175T-Q331L-M366I, has a rate of latency transition at least 72-fold slower than PAI-1 wt [29]. We observed that the peptide TVASS, which can be incorporated in two copies between s3A and s5A of PAI-1 and thereby induce substrate behaviour [40], inactivated stable PAI-1 at least 100-fold slower than PAI-1 wt (results not shown). Stable PAI-1 exhibited much less tendency than PAI-1 wt to form polymers when exposed to either of the three inactivators ANS, bis-ANS, and 1-DS, although it was less resistant to 1-DS than to ANS and bis-ANS (Figure 6). As judged by the increase of bis-ANS fluorescence induced by binding to PAI-1 [27], wt and stable PAI-1 bind bis-ANS equally well (results not shown), suggesting that the cause of the lower degree of polymerization is not a decreased inactivator binding, but rather a slower transmission of inactivator-induced conformational changes through stable PAI-1 than through PAI-1 wt.

Using native PAGE, we found that in addition to PAI-1, HCII also polymerized when exposed to 100 μM 1-DS, 5 μM bis-ANS, or 500 μM ANS, whereas we observed no, or very little, 1-DS-, bis-ANS-, or ANS-induced polymerization of α_1-PI, α_2-antiplasmin, PAI-2, ovalbumin, antithrombin III, C1-inhibitor, protease nexin 1, and α_1-ACT (Figure 7 and results not shown).

The possibility of PAI-1 co-polymerizing with other serpins was investigated by exposing 100 pM [^{32}P]PAI-1 to 1-DS in the absence or presence of 10 μM PAI-1 or another serpin. A PAI-1 concentration of 100 pM is too low to give detectable polymerization at these conditions, while 100 pM [^{32}P]PAI-1 plus micromolar concentrations of unlabelled PAI-1 polymerize readily (Figures 2 and 8). Exposure of the mixture of 100 pM [^{32}P]PAI-1 and 10 μM HCII to 1-DS also led to an induction of polymerization of the [^{32}P]PAI-1, indicating co-polymerization of the two serpins (Figure 8). Micromolar concentrations of ovalbumin, antithrombin III, α_1-PI or α_1-ACT did not support polymerization of 100 pM [^{32}P]PAI-1, although we did observe forms of [^{32}P]PAI-1, which, as judged from their migration, represented heterodimers (Figure 8 and results not shown).

Similar results were obtained with bis-ANS or ANS (results not shown).

DISCUSSION

Pathological protein polymerization, being involved in the pathogenesis of several diseases, generally implicates interaction between individual protein molecules due to conformational switching from random coil or α-helix to β-structure, mediating formation of β-sheets with strands from different molecules [41,42]. The serpin family is one class of polymerizing proteins. Several serpins, including α_1-PI, antithrombin III, PAI-2, C1-inhibitor, α_1-ACT, thyroxine binding globulin, and angiotensinogen, polymerize at temperatures around 60 °C [43–46]. Several examples of pathogenic, mutation-induced serpin polymerization are known. Pathological polymerization of α_1-PI or α_1-ACT leads to impaired secretion, formation of hepatic inclusions, and thus liver disease. Likewise, neuroserpin polymerization in the brain leads to dementia. Polymerization also leads to reduced plasma levels of α_1-PI, α_1-ACT, C1-inhibitor and antithrombin III and is accompanied by lung emphysema, angioedema and thrombosis respectively. As in other pathological protein polymerizations, all the known modes of serpin polymerization seem to involve loop-to-β-strand conversion and stabilization of β-sheets by strand insertion [22].

The PAI-1 polymers described in the present report were originally observed when studying the effect of amphipathic organochemical PAI-1 inactivators [27]. Although the polymerization process seems to compete with a more non-specific aggregation that becomes particularly evident with non-glycosylated PAI-1, and although high concentrations of ANS and high salt concentrations may lead to aggregation of latent PAI-1 and other serpins (K. E. Pedersen, unpublished work), we previously discussed a number of arguments suggesting that the polymerization process is well-ordered and not a non-specific aggregation caused by the detergent nature of the inactivators [27]. In the present study, we have substantiated this conclusion and made observations allowing us to propose a mode of PAI-1 polymerization from the three previously observed for serpins (see Introduction section).

First, thermal stability is a classical criterion for distinguishing between (*S*) and (*R*) conformations [1]. By this criterion, polymers of α_1-PI are in a classical R-conformation, resisting unfolding at temperatures above 90 °C [37], suggesting full insertion of the RCL of one molecule into β-sheet A of another molecule. The thermal stability of the PAI-1 polymers was intermediate between that of the active (*S*) form and reactive centre-cleaved PAI-1. Mutation-induced polymers of C1-inhibitor, suggested to be of the s1C type, also showed a moderate increase in thermal stability compared with monomeric C1-inhibitor [46]. Besides s1C polymerization, another possibility for explaining an intermediate stability is partial insertion of the RCL between s3A and s5A.

Secondly, stable PAI-1 polymerized slower than PAI-1 wt. Stable PAI-1 was originally isolated because of its slow latency transition [29]. We have now found that stable PAI-1 also has a slow rate of incorporation of TVASS. Together, these observations are in agreement with PAI-1 polymerization involving insertion of the RCL, as in s4A. Since s7A polymerization was observed in the crystals of exactly stable PAI-1 [19–21], the slow polymerization of the stable PAI-1 variant seems to exclude s7A polymerization, but not s1C polymerization, in the present case.

Thirdly, the ability of the polymers to slowly become reactive centre-cleaved by uPA and concomitantly depolymerized does not seem to be in agreement with an s7A mechanism, but can be explained by either an s4A or an s1C polymerization mechanism, as either the N-terminal or C-terminal part of the cleaved RCL from a polymer-terminal molecule may push out the foreign RCL as they themselves become inserted as s4A or s1C respectively.

Fourth, polymerization was associated with specific changes in proteolytic susceptibility of PAI-1, namely an inhibition of cleavage of the RCL and stimulation of cleavage of the N-terminal part of s5A and the hI–s5A loop. In latent and reactive-centre-cleaved PAI-1, these secondary structural elements are resistant to proteolysis [39]. We therefore interpret the present data as the RCL being at least partially incorporated into a β-sheet and s5A and the hI–s5A loop being flexible in the polymers. The polymerization model most readily explaining these data is insertion of the part of the RCL around P_1-P_1' into the proximal part of the cleft between s3A and s5A of another molecule, with the N-terminal part of s5A being left accessible to proteases. The fact that the cleavage site for endoproteinase Glu-C at the Glu^{342}–Ser^{343} bond remains unchanged is an argument against s1C polymerization, as this implies partial intramolecular insertion of the RCL between s3A and s5A (Figure 1B), and this type of RCL insertion is associated with protection of that bond [39].

In addition, we previously reported that latent and reactive-centre-cleaved PAI-1 displayed a much weaker binding of ANS than active PAI-1, whereas polymerized PAI-1 maintained strong ANS binding [27]. This observation provides an argument that polymerization does not involve full insertion of the RCL as s4A. In fact, the traditional way of demonstrating s4A polymerization, namely inhibition of polymerization by RCL peptides, could not be used in the present case, as incorporation of TVASS in two copies between s3A and s5A [40] prevented binding of the polymerization-inducing ligands (results not shown).

Taken together, our results are in best agreement with an s4A polymerization mechanism, in which ligand binding induces separation of s3A and s5A, allowing partial insertion of the RCL of one molecule into the upper part of the cleft between s3A and s5A of another molecule while the lower part of s5A and the hI–s5A loop remain flexible. This model is compatible with all our observations, while s1C- or s7A-polymerization mechanisms or a full insertion mechanism seem to be in disagreement with one or more of the observations. The proposed model is also attractive from the point of view that it does not predict that polymerization needs translocation of hF and the hF–s3A loop. We have viewed our observations in relation to the three known serpin polymerization mechanisms, but we cannot exclude the possibility that alternative, unknown polymerization mechanisms can occur.

Interestingly, among a number of serpins tested, only HCII was found to polymerize upon exposure to the negatively charged, amphipathic compounds tested here. The capability of PAI-1 and HCII to co-polymerize must imply that the RCL of one of these serpins is able into insert into a sheet of the other and that the mechanisms for polymerization of each individual serpin are similar. In fact, the recently published X-ray crystal structure of HCII [47] is compatible with a hydrophobic cavity in the flexible joint region similar to that in PAI-1. Antithrombin III and α_1-PI have corresponding hydrophobic cavities of similar volumes [25], so we must propose that the existence of the hydrophobic cavity is a necessary, but not sufficient, condition for ligand-induced polymerization. The observed hetero-dimerization of PAI-1 with ovalbumin must be caused by the effect of the ligands on PAI-1. A possible mechanism for hetrodimerization is a ligand-induced sliding apart of s3A and s5A of PAI-1, allowing insertion of ovalbumin's RCL.

The present work should also be viewed in the context of PAI-1 being a risk factor in both cancer spread [6] and

development of cardiovascular diseases [48], and the ensuing interest in development of PAI-1-inactivating drugs. Induction of polymerization of PAI-1 is an undesired feature of a drug, due to the potentially toxic effects of such polymers. At physiological blood plasma concentrations of PAI-1 (around 100 pM), polymerization is expected to occur very slowly, but measurements of PAI-1 in cells with high expression [49], or blood platelets [50], allow a rough estimation of intra-vesicular PAI-1 concentrations to the high nanomolar or micromolar range, at which polymerization occurs rapidly.

We thank Ida Thøgersen and Tanja Christiansen for very skilled technical assistance. This work was supported by the Danish Cancer Society, the Danish Natural Science Research Council, the Danish Research Agency, the Danish Cancer Research Foundation, and the Novo Nordisk Foundation.

REFERENCES

1 Carrell, R. W. and Owen, M. C. (1985) Plakalbumin, α1-antitrypsin, antithrombin and the mechanism of inflammatory thrombosis. Nature (London) **317**, 730–732
2 Irving, J. A., Pike, R. N., Lesk, A. M. and Whisstock, J. C. (2000) Phylogeny of the serpin superfamily: implications of patterns of amino acid conservation for structure and function. Genome Res. **10**, 1845–1864
3 Huber, R. and Carrell, R. W. (1989) Implications of the three-dimensional structure of α1-antitrypsin for structure and function of serpins. Biochemistry **28**, 8951–8966
4 Gils, A. and Declerck, P. J. (1998) Structure–function relationships in serpins: current concepts and controversies. Thromb. Haemostasis **80**, 531–541
5 Ye, S. and Goldsmith, E. J. (2001) Serpins and other covalent protease inhibitors. Curr. Opin. Struct. Biol. **11**, 740–745
6 Wind, T., Hansen, M., Jensen, J. K. and Andreasen, P. A. (2002) The molecular basis for anti-proteolytic and non-proteolytic functions of plasminogen activator inhibitor type-1: roles of the reactive centre loop, the shutter region, the flexible joint region and the small serpin fragment. Biol. Chem. **383**, 21–36
7 Ye, S., Cech, A. L., Belmares, R., Bergstrom, R. C., Tong, Y., Corey, D. R., Kanost, M. R. and Goldsmith, E. J. (2001) The structure of a Michaelis serpin–protease complex. Nat. Struct. Biol. **8**, 979–983
8 Lawrence, D. A., Ginsburg, D., Day, D. E., Berkenpas, M. B., Verhamme, I. M., Kvassman, J. O. and Shore, J. D. (1995) Serpin-protease complexes are trapped as stable acyl-enzyme intermediates. J. Biol. Chem. **270**, 25309–25312
9 Shore, J. D., Day, D. E., Francis-Chmura, A. M., Verhamme, I., Kvassman, J., Lawrence, D. A. and Ginsburg, D. (1995) A fluorescent probe study of plasminogen activator inhibitor-1. Evidence for reactive center loop insertion and its role in the inhibitory mechanism. J. Biol. Chem. **270**, 5395–5398
10 Wilczynska, M., Fa, M., Ohlsson, P. I. and Ny, T. (1995) The inhibition mechanism of serpins. Evidence that the mobile reactive center loop is cleaved in the native protease-inhibitor complex. J. Biol. Chem. **270**, 29652–29655
11 Egelund, R., Rodenburg, K. W., Andreasen, P. A., Rasmussen, M. S., Guldberg, R. E. and Petersen, T. E. (1998) An ester bond linking a fragment of a serine proteinase to its serpin inhibitor. Biochemistry **37**, 6375–6379
12 Egelund, R., Petersen, T. E. and Andreasen, P. A. (2001) A serpin-induced extensive proteolytic susceptibility of urokinase-type plasminogen activator implicates distortion of the proteinase substrate-binding pocket and oxyanion hole in the serpin inhibitory mechanism. Eur. J. Biochem. **268**, 673–685
13 Huntington, J. A., Read, R. J. and Carrell, R. W. (2000) Structure of a serpin-protease complex shows inhibition by deformation. Nature (London) **407**, 923–926
14 Lawrence, D. A., Olson, S. T., Muhammad, S., Day, D. E., Kvassman, J. O., Ginsburg, D. and Shore, J. D. (2000) Partitioning of serpin-proteinase reactions between stable inhibition and substrate cleavage is regulated by the rate of serpin reactive center loop insertion into β-sheet A. J. Biol. Chem. **275**, 5839–5844
15 Mottonen, J., Strand, A., Symersky, J., Sweet, R. M., Danley, D. E., Geoghegan, K. F., Gerard, R. D. and Goldsmith, E. J. (1992) Structural basis of latency in plasminogen activator inhibitor-1. Nature (London) **355**, 270–273
16 Carrell, R. W., Stein, P. E., Fermi, G. and Wardell, M. R. (1994) Biological implications of a 3 Å structure of dimeric antithrombin. Structure **2**, 257–270
17 Jin, L., Abrahams, J. P., Skinner, R., Petitou, M., Pike, R. N. and Carrell, R. W. (1997) The anticoagulant activation of antithrombin by heparin. Proc. Natl. Acad. Sci. U.S.A. **94**, 14683–14688
18 Schreuder, H. A., de Boer, B., Dijkema, R., Mulders, J., Theunissen, H. J., Grootenhuis, P. D. and Hol, W. G. (1994) The intact and cleaved human antithrombin III complex as a model for serpin-proteinase interactions. Nat. Struct. Biol. **1**, 48–54
19 Sharp, A. M., Stein, P. E., Pannu, N. S., Carrell, R. W., Berkenpas, M. B., Ginsburg, D., Lawrence, D. A. and Read, R. J. (1999) The active conformation of plasminogen activator inhibitor 1, a target for drugs to control fibrinolysis and cell adhesion. Structure Fold. Des. **7**, 111–118
20 Nar, H., Bauer, M., Stassen, J. M., Lang, D., Gils, A. and Declerck, P. J. (2000) Plasminogen activator inhibitor 1. Structure of the native serpin, comparison to its other conformers and implications for serpin inactivation. J. Mol. Biol. **297**, 683–695
21 Stout, T. J., Graham, H., Buckley, D. I. and Matthews, D. J. (2000) Structures of active and latent PAI-1: a possible stabilizing role for chloride ions. Biochemistry **39**, 8460–8469
22 Lomas, D. A. and Carrell, R. W. (2002) Human genetics and disease: Serpinopathies and the conformational dementias. Nat. Rev. Genet. **3**, 759–768
23 Huntington, J. A., Pannu, N. S., Hazes, B., Read, R. J., Lomas, D. A. and Carrell, R. W. (1999) A 2.6 Å structure of a serpin polymer and implications for conformational disease. J. Mol. Biol. **293**, 449–455
24 Dunstone, M. A., Dai, W., Whisstock, J. C., Rossjohn, J., Pike, R. N., Feil, S. C., Le Bonniec, B. F., Parker, M. W. and Bottomley, S. P. (2000) Cleaved antitrypsin polymers at atomic resolution. Protein Sci. **9**, 417–420
25 Elliott, P. R., Pei, X. Y., Dafforn, T. R. and Lomas, D. A. (2000) Topography of a 2.0 Å structure of α1-antitrypsin reveals targets for rational drug design to prevent conformational disease. Protein Sci. **9**, 1274–1281
26 Björquist, P., Ehnebom, J., Inghardt, T., Hansson, L., Lindberg, M., Linschoten, M., Strömqvist, M. and Deinum, J. (1998) Identification of the binding site for a low-molecular-weight inhibitor of plasminogen activator inhibitor type 1 by site-directed mutagenesis. Biochemistry **37**, 1227–1234
27 Egelund, R., Einholm, A. P., Pedersen, K. E., Nielsen, R. W., Christensen, A., Deinum, J. and Andreasen, P. A. (2001) A regulatory hydrophobic area in the flexible joint region of plasminogen activator inhibitor-1, defined with fluorescent activity-neutralizing ligands. Ligand-induced serpin polymerization. J. Biol. Chem. **276**, 13077–13086
28 Munch, M., Heegaard, C. W. and Andreasen, P. A. (1993) Interconversions between active, inert and substrate forms of denatured/refolded type-1 plasminogen activator inhibitor. Biochim. Biophys. Acta **1202**, 29–37
29 Berkenpas, M. B., Lawrence, D. A. and Ginsburg, D. (1995) Molecular evolution of plasminogen activator inhibitor-1 functional stability. EMBO J. **14**, 2969–2977
30 Hansen, M., Busse, M. N. and Andreasen, P. A. (2001) Importance of the amino-acid composition of the shutter region of plasminogen activator inhibitor-1 for its transitions to latent and substrate forms. Eur. J. Biochem. **268**, 6274–6283
31 von Heijne, G. (1984) How signal sequences maintain cleavage specificity. J. Mol. Biol. **173**, 243–251
32 Jensen, J. K., Wind, T. and Andreasen, P. A. (2002) The vitronectin binding area of plasminogen activator inhibitor-1, mapped by mutagenesis and protection against an inactivating organochemical ligand. FEBS Lett. **521**, 91–94
33 Wind, T., Jensen, M. A. and Andreasen, P. A. (2001) Epitope mapping for four monoclonal antibodies against human plasminogen activator inhibitor type-1: implications for antibody-mediated PAI-1-neutralization and vitronectin-binding. Eur. J. Biochem. **268**, 1095–1106
34 Schägger, H. and von Jagow, G. (1991) Blue native electrophoresis for isolation of membrane protein complexes in enzymatically active form. Anal. Biochem. **199**, 223–231
35 Guex, N. and Peitsch, M. C. (1997) SWISS-MODEL and the Swiss-PdbViewer: an environment for comparative protein modeling. Electrophoresis **18**, 2714–2723
36 Munch, M., Heegaard, C., Jensen, P. H. and Andreasen, P. A. (1991) Type-1 inhibitor of plasminogen activators. Distinction between latent, activated and reactive centre-cleaved forms with thermal stability and monoclonal antibodies. FEBS Lett. **295**, 102–106
37 Lomas, D. A., Evans, D. L., Stone, S. R., Chang, W. S. and Carrell, R. W. (1993) Effect of the Z mutation on the physical and inhibitory properties of α1-antitrypsin. Biochemistry **32**, 500–508
38 Egelund, R., Schousboe, S. L., Sottrup-Jensen, L., Rodenburg, K. W. and Andreasen, P. A. (1997) Type-1 plasminogen-activator inhibitor – conformational differences between latent, active, reactive-centre-cleaved and plasminogen-activator-complexed forms, as probed by proteolytic susceptibility. Eur. J. Biochem. **248**, 775–785
39 Kjøller, L., Martensen, P. M., Sottrup-Jensen, L., Justesen, J., Rodenburg, K. W. and Andreasen, P. A. (1996) Conformational changes of the reactive-centre loop and β-strand 5A accompany temperature-dependent inhibitor-substrate transition of plasminogen-activator inhibitor 1. Eur. J. Biochem. **241**, 38–46
40 Xue, Y., Björquist, P., Inghardt, T., Linschoten, M., Musil, D., Sjölin, L. and Deinum, J. (1998) Interfering with the inhibitory mechanism of serpins: crystal structure of a complex formed between cleaved plasminogen activator inhibitor type 1 and a reactive-centre loop peptide. Structure **6**, 627–636

41 Dumery, L., Bourdel, F., Soussan, Y., Fialkowsky, A., Viale, S., Nicolas, P. and Reboud-Ravaux, M. (2001) β-Amyloid protein aggregation: its implication in the physiopathology of Alzheimer's disease. Pathol. Biol. (Paris) **49**, 72–85
42 Lücking, C. B. and Brice, A. (2000) α-Synuclein and Parkinson's disease. Cell. Mol. Life Sci. **57**, 1894–1908
43 Mast, A. E., Enghild, J. J. and Salvesen, G. (1992) Conformation of the reactive site loop of α1-proteinase inhibitor probed by limited proteolysis. Biochemistry **31**, 2720–2728
44 Preissner, K. T. (1993) Self-association of antithrombin III relates to multimer formation of thrombin-antithrombin III complexes. Thromb. Haemostasis **69**, 422–429
45 Mikus, P., Urano, T., Liljeström, P. and Ny, T. (1993) Plasminogen-activator inhibitor type 2 (PAI-2) is a spontaneously polymerising SERPIN. Biochemical characterisation of the recombinant intracellular and extracellular forms. Eur. J. Biochem. **218**, 1071–1082
46 Patston, P. A., Hauert, J., Michaud, M. and Schapira, M. (1995) Formation and properties of C1-inhibitor polymers. FEBS Lett. **368**, 401–404

Received 2 December 2002/24 March 2003; accepted 26 March 2003
Published as BJ Immediate Publication 26 March 2003, DOI 10.1042/ BJ20021868

47 Baglin, T. P., Carrell, R. W., Church, F. C., Esmon, C. T. and Huntington, J. A. (2002) Crystal structures of native and thrombin-complexed heparin cofactor II reveal a multistep allosteric mechanism. Proc. Natl. Acad. Sci. U.S.A. **99**, 11079–11084
48 Huber, K., Christ, G., Wojta, J. and Gulba, D. (2001) Plasminogen activator inhibitor type-1 in cardiovascular disease. Status report (2001) Thromb. Res. **103**, S7–S19
49 Andreasen, P. A., Pyke, C., Riccio, A., Kristensen, P., Nielsen, L. S., Lund, L. R., Blasi, F. and Danø, K. (1987) Plasminogen activator inhibitor type 1 biosynthesis and mRNA level are increased by dexamethasone in human fibrosarcoma cells. Mol. Cell. Biol. **7**, 3021–3025
50 Booth, N. A., Simpson, A. J., Croll, A., Bennett, B. and MacGregor, I. R. (1988) Plasminogen activator inhibitor (PAI-1) in plasma and platelets. Br. J. Haematol. **70**, 327–333
51 Andreasen, P. A., Riccio, A., Welinder, K. G., Douglas, R., Sartorio, R., Nielsen, L. S., Oppenheimer, C., Blasi, F. and Danø, K. (1986) Plasminogen activator inhibitor type-1: reactive center and amino-terminal heterogeneity determined by protein and cDNA sequencing. FEBS Lett. **209**, 213–218